WIRELESS COMMUNICATIONS AND MOBILE COMPUTING
Wirel. Commun. Mob. Comput. **00**: 1–17 (0000)
Published online in Wiley InterScience
(www.interscience.wiley.com) DOI: 10.1002/wcm.0000

An Evolutionary Spectrum Approach to Modeling Non-stationary Fading Channels

Qing Wang[1], Dapeng Wu[2*,†] and Pingyi Fan[3]

[1] *National Computer network Emergency Response technical Team/Coordination Center of China (CNCERT/CC), Beijing, China 100029, and Department of Electronic Engineering, Tsinghua University, Beijing, China 100084.*
[2] *Department of Electrical and Computer Engineering, University of Florida, Gainesville, FL 32611.*
[3] *Department of Electronic Engineering, Tsinghua University, Beijing, China 100084 and National Mobile Communications Research Laboratory, Southeast University, China 210096.*

Summary

To evaluate mobile communication systems, it is important to develop accurate and concise fading channel models. However, fading encountered in mobile communication is usually non-stationary, and the existing methods can only model quasi-stationary or piecewise-stationary fading instead of general non-stationary fading. To address this, this paper proposes an evolutionary-spectrum (ES) based approach to modeling non-stationary fading channels. Our ES approach is more general than the existing piecewise-stationary models, and is capable of characterizing a general non-stationary fading channel that has an arbitrary evolutionary spectrum (or time-varying power spectral density); our ES approach is parsimonious, and is also able to generate stationary fading processes. As an example, we show how to apply our ES approach to generating stationary and non-stationary correlated Nakagami-m fading channel processes. Simulation results show that the evolutionary spectrum of the channel gain process produced by our ES-based channel model agrees well with the user-specified evolutionary spectrum, indicating the accuracy of our ES-based channel model. Copyright © 0000 John Wiley & Sons, Ltd.

KEY WORDS: Channel modeling, non-stationarity, evolutionary spectrum, mobile communication, fading channel.

1. Introduction

Time-varying fading channels pose a great challenge to mobile communication. To evaluate the performance of mobile communication systems, it is important to develop accurate and parsimonious fading channel models. Existing channel models can be classified into two categories: large-scale path loss and small-scale fading. Large-scale path loss models, also called propagation models, characterize the underlying physical mechanisms (*i.e.*, reflection, diffraction, scattering) for specific paths. These models specify signal attenuation as a function of distance, which is affected by prominent terrain contours (buildings, hills, forests, etc.) between the transmitter and the receiver. Path loss models describe the mean signal attenuation vs. distance in a deterministic fashion (*e.g.*, nth-power law [1]), and also the statistical variation about the mean (*e.g.*, log-normal distribution [1]).

Small-scale fading models describe the characteristics of generic radio paths in a statistical fashion.

*Correspondence to: Prof.Dapeng Wu, Department of Electrical and Computer Engineering, University of Florida, Gainesville, FL 32611.
†E-mail: wu@ece.ufl.edu

Prepared using wcmauth.cls *[Version: 2007/01/09 v1.00]*

Small-scale fading refers to the dramatic changes in signal amplitude and phase that can be experienced as a result of small changes (as small as a half-wavelength) in the spatial separation between the receiver and the transmitter [2]. Small-scale fading can be slow or fast, depending on the Doppler rate. Small-scale fading can also be flat or frequency-selective, depending on the delay spread of the channel. The statistical time-varying nature of the envelope of a flat-fading signal is characterized by distributions such as Rayleigh, Ricean, Nakagami, etc. [1]. Uncorrelated scattering is often assumed, to extend these distributions to the frequency-selective case. The large-scale path loss and small-scale fading together characterize the received signal power over a wide range of distances.

However, small-scale fading encountered in mobile communication is usually non-stationary, and the existing methods can only model quasi-stationary or piecewise-stationary fading channels [3, 4, 5, 6, 7, 8] instead of general non-stationary fading channels. To address this, this paper proposes an evolutionary-spectrum (ES) [9] based approach to modeling non-stationary fading channels. Our ES approach is more general than the existing piecewise-stationary models, and is capable of characterizing a general non-stationary fading channel that has an arbitrary evolutionary spectrum (which represents time-varying power spectral density); our ES approach is parsimonious, and is also able to generate stationary fading processes. As an example, we show how to apply our ES approach to generating stationary and non-stationary correlated Nakagami-m fading channels. Simulation results show that the evolutionary spectrum of the channel gain process produced by our ES-based channel model agrees well with the user-specified evolutionary spectrum; this indicates the accuracy of our ES-based channel model.

In contrast, in the near few years, with respect to the measurement-based V2V propagation channel models given by [10][11] in which we note that, first, the LOS (Line Of Sight), diffuse scatters and discrete scatters are all considered. Specifically, (*i*) diffuse scatterers are modeled as GSCM (Geometry-based Stochastic Channel Model), i.e., with random complex Gaussian amplitudes; and (*ii*) the amplitude of the LOS and the discrete scatterers are modeled according to a Rayleigh distribution. In addition to fading, the Doppler spectrum can be large and hence can change rapidly with time. Second, for a practical mobile scene, the mobile fading channel may be rather complicated. To model it accurately, several measurement-based algorithms and empirical modeling approaches have been proposed (See, for example, [10][11]). Such approaches may be more accurate. However, the loss of simple closed form solution of the channel fading description makes the analysis of the system performance quite difficult. This is because the modeling steps for these approaches completely rely on the realtime estimation of the channel response. Therefore, our approach overcomes this and provides both the feasibility of theoretical derivation and modeling accuracy.

The rest of the paper is organized as follows. In Section 2, we review the ES theory [9]. Section 3 presents our ES-based approach to modeling non-stationary fading channels. In Section 4, we show how to apply our ES approach to generating stationary and non-stationary correlated Nakagami-m fading channels. Section 5 shows simulation results to demonstrate the accuracy of our ES-based channel model. Section 6 concludes the paper.

2. Review of the Evolutionary Spectrum Theory

We first review the spectral representation of a stationary process $X(t)$ as follows [9, page 246]

$$X(t) = \int_{-\infty}^{+\infty} e^{j\omega t} d\mathcal{Z}(\omega) \tag{1}$$

where $\mathcal{Z}(\omega)$ is an orthogonal process. The auto-correlation function of $X(t)$ admits the following spectral representation

$$R(s,t) = E[X(s)X(t)] = \int_{-\infty}^{+\infty} e^{j\omega(t-s)} d\mathcal{H}(\omega) \tag{2}$$

where $E[|d\mathcal{Z}(\omega)|^2] = d\mathcal{H}(\omega)$, and $\mathcal{H}(\omega)$ is the integrated power spectrum of $X(t)$; the derivative of $\mathcal{H}(\omega)$ with respect to (w.r.t.) ω is the power spectral density of $X(t)$. If we let $t = s$, then we get the power of $X(t)$ as below

$$E[X^2(t)] = R(t,t) = \int_{-\infty}^{+\infty} d\mathcal{H}(\omega) \tag{3}$$

According to Parzen's work [12, 13], the auto-correlation function $R(s,t)$ of a non-stationary process $X(t)$ can be represented in a form similar to (2), provided that we replace the functions $\{e^{j\omega t}\}$ by a more general family of functions $\{\phi_t(\omega)\}$. Specifically, there exist a family $\mathcal{F}$ of functions

DOI: 10.1002/wcm

$\{\phi_t(\omega)\}$ ($\omega \in \mathbb{R}$) indexed by t and a measure $\mu(\omega)$ ($\omega \in \mathbb{R}$) such that for any $s \in \mathbb{R}$ and $t \in \mathbb{R}$, the auto-correlation function $R(s,t)$ admits the following representation:

$$R(s,t) = \int_{-\infty}^{+\infty} \phi_s^*(\omega)\phi_t(\omega)d\mu(\omega) \tag{4}$$

where $\phi_s^*(\omega)$ is complex conjugate of $\phi_s(\omega)$. In addition, in order for the variance of $\{X(t)\}$ to be finite for each t, $\phi_t(\omega)$ must be quadratically integrable w.r.t. the measure $\mu(\omega)$ for each t; in other words, this is the condition of $\{X(t)\}$ having finite instantaneous power at each t.

Similarly, the general process $X(t)$, which can be non-stationary or stationary, admits the following representation:

$$X(t) = \int_{-\infty}^{+\infty} \phi_t(\omega)d\mathcal{Z}(\omega) \tag{5}$$

where $\mathcal{Z}(\omega)$ is a stochastic process with $E[|d\mathcal{Z}(\omega)|^2] = d\mu(\omega)$. The measure $\mu(\omega)$ here plays the same role as the integrated power spectrum $\mathcal{H}(\omega)$ of a stationary process. If $X(t)$ is a stationary process, a choice for a family $\mathcal{F}$ of functions $\{\phi_t(\omega)\}$ is the family of complex exponential functions, i.e., $\phi_t(\omega) = e^{j\omega t}$.

Next, we describe a family $\mathcal{F}$ of functions $\{\phi_t(\omega)\}$ for a non-stationary process as below [9]:

$$\phi_t(\omega) = A_t(\omega)e^{j\theta(\omega)t} \tag{6}$$

where for each fixed ω, the modulus of the Fourier transform of t-function $A_t(\omega)$, denoted by $|\mathcal{K}_\omega(\theta)|$, has an absolute maximum at frequency $\theta = 0$. Hence, for each fixed ω, we may regard $\phi_t(\omega)$ as an amplitude modulated (AM) signal, i.e., $A_t(\omega)$ modulates $e^{j\theta(\omega)t}$, where $e^{j\theta(\omega)t}$ can be regarded as a sinusoid of frequency $\theta(\omega)$. We now formalize this approach in the following definition [9, page 823].

Definition 1 *The function of t, $\phi_t(\omega)$, will be said to be an oscillatory function if, for some (necessarily unique) $\theta(\omega)$, it may be written in the form (6) where $A_t(\omega)$ is of the form*

$$A_t(\omega) = \int_{-\infty}^{+\infty} e^{j\theta t}d\mathcal{K}_\omega(\theta) \tag{7}$$

with $|d\mathcal{K}_\omega(\theta)|$ having an absolute maximum at $\theta = 0$.

Actually, $\mathcal{K}_\omega(\theta)$ is the integrated frequency spectrum of the t-function $A_t(\omega)$ for any fixed ω, over the frequency axis θ.

The function $A_t(\omega)$ can be regarded as the envelope of $\phi_t(\omega)$. If, further, the family $\{\phi_t(\omega)\}$ is such that $\theta(\omega)$ is the single-valued function of ω (i.e., if no two distinct members of this family have Fourier transforms whose maxima occur at the same point), then we may transform the variable in the integral in (4) from ω to $\theta(\omega)$, and by suitably redefining $A_t(\omega)$ and the measure $\mu(\omega)$, we can write

$$\begin{aligned} R(s,t) &= \int_{-\infty}^{+\infty} A_s^*(\omega)A_t(\omega)e^{j\omega(t-s)}d\mu(\omega) \\ &= \int_{-\infty}^{+\infty} A_s^*(\omega)A_t(\omega)e^{j\omega(t-s)}h(\omega)d\omega \end{aligned} \tag{8}$$

where $d\mu(\omega) = h(\omega)d\omega$, and correspondingly,

$$X(t) = \int_{-\infty}^{+\infty} A_t(\omega)e^{j\omega t}d\mathcal{Z}(\omega) \tag{9}$$

where $E[|d\mathcal{Z}(\omega)|^2] = d\mu(\omega)$. Then, we have

$$E[X^2(t)] = R(t,t) = \int_{-\infty}^{+\infty} |A_t(\omega)|^2 d\mu(\omega) \tag{10}$$

Since $E[X^2(t)]$ may be interpreted as the power of $X(t)$ at time t, (10) gives a decomposition of power, in which the contribution from frequency ω is $|A_t(\omega)|^2 d\mu(\omega)$. This leads to the definition of *Evolutionary Spectrum* as follows[9, page 824].

Definition 2 *Let $\mathcal{F}$ denote a particular family of oscillatory functions, $\{\phi_t(\omega)\} \equiv \{A_t(\omega)e^{j\omega t}\}$, and let $X(t)$ be a process having a representation of the form (9) in terms of the family $\mathcal{F}$. We define the evolutionary power spectrum at time t with respect to the family $\mathcal{F}$, $d\mathcal{H}_t(\omega)$, by*

$$d\mathcal{H}_t(\omega) = |A_t(\omega)|^2 d\mu(\omega) \tag{11}$$

and $|A_t(\omega)|^2 h(\omega)$ is called evolutionary spectral density function.

Note that when $X(t)$ is stationary and $\mathcal{F}$ is chosen to be the family of complex exponential functions $\{e^{j\omega t}\}$, the Evolutionary Spectrum $d\mathcal{H}_t(\omega)$ reduces to conventional power spectrum.

DOI: 10.1002/wcm

3. Evolutionary Spectrum Approach to Modeling Non-stationary Fading Channels

This section is organized as follows. In Section 3.1, we present an evolutionary spectrum approach to modeling non-stationary fading channels. Section 3.2 describes an evolutionary spectrum approach to simulating a non-stationary fading process that matches a given measured channel gain process.

3.1. Evolutionary Spectrum Approach to Channel Modeling

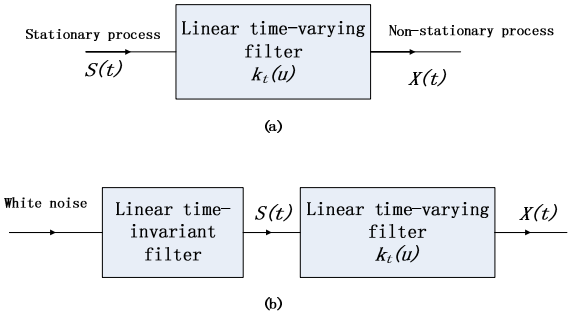

Fig. 1. The ES-based channel model

Fig. 1(a) shows a system that generates a non-stationary fading process using evolutionary spectrum. As shown in Fig. 1(a), the ES-based channel model is characterized by $S(t)$, $k_t(u)$ and $X(t)$, where input $S(t)$ is a stationary stochastic process, $k_t(u)$ is the impulse response of the linear time varying filter, and output $X(t)$ is a non-stationary fading process. Thus, our key idea is that, to model a non-stationary process $X(t)$, we need to find a stationary process $S(t)$ as stimulus and a proper time varying impulse response $k_t(u)$, and then use the linear time varying system in Fig. 1(a) to generate the non-stationary process $X(t)$.

Actually, in signal processing, the same approach as that in Fig. 1(a) has been used to generate a non-stationary process [9]. However, in wireless channel modeling, this approach has not been explored previously; this approach is able to produce a more general non-stationary fading process than the existing piecewise stationary channel models such as the VTFAR (*Vector Time-Frequency AR*) model [14]. Moreover, the model in Fig. 1(a) facilitates the generation of a non-stationary fading process that matches channel measurements, i.e., the channel gains measured from a realistic channel can help determine $k_t(u)$ and the power spectrum density of $S(t)$, and then the fading process generated by the model in Fig. 1(a) will have similar statistical properties to those of the channel measurements. This trace-driven simulator is particularly useful for evaluating the performance of a communication system.

Next, we explain why a non-stationary channel can be modeled by the system shown in Fig. 1(a). Let $X(t)$ be of the form (9) with the evolutionary spectrum equal to $|A_t(\omega)|^2 d\mu(\omega)$. For fixed t, we take inverse Fourier transform of $A_t(\omega)$ w.r.t. ω, i.e.,

$$k_t(u) = \int_{-\infty}^{+\infty} A_t(\omega) e^{j\omega u} d\omega. \tag{12}$$

Its forward Fourier transform is

$$A_t(\omega) = \int_{-\infty}^{+\infty} k_t(u) e^{-j\omega u} du \tag{13}$$

Note that parameter u is a new variable different from time t. Actually, u is considered as the time lapse from epoch t. Substituting $A_t(\omega)$ in (9) by its expression in (13), we obtain

$$X(t) = \int_{-\infty}^{+\infty} S(t-u) k_t(u) du \tag{14}$$

where $S(t) = \int_{-\infty}^{+\infty} e^{j\omega t} d\mathcal{Z}(\omega)$. So $S(t)$ is a stationary process with power spectrum $d\mu(\omega)$. According to (14), $X(t)$ can be generated by a linear time varying filter whose impulse response is $k_t(u)$, with input $S(t)$, which is a stationary process with power spectrum $d\mu(\omega)$. This explains why a non-stationary fading channel can be modeled by the system shown in Fig. 1(a).

In summary, our ES-based channel model can be described as below: given the evolutionary spectrum of the channel $|A_t(\omega)|^2 d\mu(\omega)$, we can use $A_t(\omega)$ to obtain $k_t(u)$ via (12), and use the power spectrum $d\mu(\omega)$ to generate stationary process $S(t)$; i.e., a non-stationary fading channel is modeled by the system shown in Fig. 1(b), where the linear time-invariant filter has a frequency response of $\sqrt{d\mu(\omega)}$.

3.2. ES-based Channel Simulator

Algorithm 1 shows an ES-based channel simulator that generates a non-stationary fading process, given a user-specified time-varying autocorrelation function $R(s,t)$.

Algorithm 1 *ES-based channel simulator.*

1. ***Input***: $R(s,t)$

DOI: 10.1002/wcm

2. *Decompose $R(s,t)$ and obtain $A_t(\omega)$ and $h(\omega)$ that satisfy (8).*
3. *Computer the inverse Fourier transform of $A_t(\omega)$, i.e., (12), and obtain $k_t(u)$.*
4. *Given $h(\omega)$ and $k_t(u)$, generate $X(t)$ via the system shown in Fig. 1(b).*
5. ***Output**: $X(t)$.*

In Step 2 of Algorithm 1, there are two cases for decomposition of $R(s,t)$. The first case is that the closed form of $A_t(\omega)$ exists and can be easily obtained by decomposing $R(s,t)$; in this case, we can directly obtain $A_t(\omega)$ by the decomposition. An example of this case is given in Section 4.2. The second case is that the closed form of $A_t(\omega)$ is very difficult to identify or does not exist; in this case, we can use some numerical methods such as the joint frequency discrimination and amplitude demodulation strategy to extract $A_t(\omega)$ for each fixed value of ω.

If the channel gain measurements of a fading channel (rather than $R(s,t)$) are given, we can first estimate $R(s,t)$ from the channel gain measurements; then use the estimated $R(s,t)$ as the input and run Algorithm 1 to produce a non-stationary fading process, which shares similar $R(s,t)$ to that of the measured channel.

4. ES-based Model for Correlated Nakagami-m Fading Channels

In Section 3, we present an evolutionary spectrum approach to modeling non-stationary fading channels. In this section, as an example, we show how to apply our ES approach to generating stationary and non-stationary *correlated Nakagami-m fading* channel processes. This section is organized as follows. In Section 4.1, we derive $R(s,t)$ of a non-stationary Nakagami-m fading channel. In Section 4.2, we use the formula of $R(s,t)$ derived in Section 4.1 to design an ES-based channel simulator that generates a *non-stationary* correlated Nakagami-m fading process. Section 4.3 presents an ES-based channel simulator that generates a *stationary* correlated Nakagami-m fading process.

4.1. Auto-correlation Function of a Non-stationary Correlated Nakagami-m Fading Process

In this section, we derive the auto-correlation function $R(s,t)$ of a non-stationary correlated Nakagami-m fading channel. In this paper, we only consider the case where m is a positive integer.

Proposition 1 *Let $X(t)$ ($t \in \mathbb{R}$) denote a Nakagami-m fading process. Assume that for any $s \in \mathbb{R}$ and $t \in \mathbb{R}$ ($s \neq t$), the joint probability density function (pdf) of $X(s)$ and $X(t)$ is given by [15, 16]*

$$f(x,y) = \frac{4(xy)^m e^{-(\eta_y x^2+\eta_x y^2)/(\eta_x\eta_y(1-\rho))}}{\Gamma(m)\eta_x\eta_y(1-\rho)(\eta_x\eta_y\rho)^{(m-1)/2}} \cdot I_{m-1}\left(\frac{2\sqrt{\rho}xy}{\sqrt{\eta_x\eta_y}(1-\rho)}\right), \tag{15}$$

where (for simplicity of notation) $x = X(s)$ and $y = X(t)$; $x \geq 0$; $y \geq 0$; $m \geq \frac{1}{2}$; $\eta_x = E[x^2]/m$; $\eta_y = E[y^2]/m$; $\rho = Cov(x^2, y^2)/\sqrt{var(x^2)var(y^2)}$, which is the power cross correlation coefficient; $\rho \neq 0$; $\rho \neq 1$; and $I_k(\cdot)$ is the modified Bessel function of the k-th order. Then the auto-correlation function $R(s,t)$ of $X(t)$ is given by

$$R(s,t) = \frac{\pi\sqrt{\eta_s\eta_t}(1-\rho(s,t))^{m+1}}{4}\left[\frac{(2m-1)!!}{(2m-2)!!}\right]^2 \cdot {}_2F_1\left(m+\frac{1}{2}, m+\frac{1}{2}; m; \rho(s,t)\right), \tag{16}$$

where ${}_2F_1(\cdot,\cdot;\cdot;\cdot)$ is a hypergeometric function [17]; $\eta_s = E[X^2(s)]/m$; $\eta_t = E[X^2(t)]/m$; and $\rho(s,t) = \frac{Cov(X^2(s),X^2(t))}{\sqrt{var(X^2(s))var(X^2(t))}}$.

A proof for Proposition 1 is given in Appendix .1.

By using the expression of ${}_2F_1(m+\frac{1}{2}, m+\frac{1}{2}; m; \rho)$ and using the Taylor series expansion of $(1-\rho)^m$, i.e., $(1-\rho)^m = \sum_{k=0}^{m}(-1)^k C_m^k \rho^k$ where $\rho \neq 1$ and $C_m^k = \frac{m!}{k!(m-k)!}$, we can further simplify (16) and obtain

$$R(s,t) = \frac{\pi\sqrt{\eta_s\eta_t}}{4}\left[\frac{(2m-1)!!}{(2m-2)!!}\right]^2 \sum_{k=0}^{\infty} C(m,k)\rho^k(s,t), \tag{17}$$

where $C(m,k)$ is defined in Table I, in which $P(m,k)$ and $Q(m,k)$ are given by

$$P(m,k) = \begin{cases} (-1)^k C_{m+1}^k, & k \leq m+1, \quad (18) \\ 0, & k \geq m+2 \quad (18') \end{cases}$$

$$Q(m,k) = \frac{\{[2(m+k)-1]!!\}^2(2m-2)!!}{(2k)!![2(m+k-1)]!![(2m-1)!!]^2}, \quad k = 0, 1, \cdots, \infty. \tag{19}$$

(17) can be further simplified. First, $C(m,k)$ is a positive and dramatically decreasing sequence of

DOI: 10.1002/wcm

Table I. The expression of $C(m,k)$

$$
\begin{aligned}
C(m,0) &= P(m,0)Q(m,0)\\
C(m,1) &= P(m,0)Q(m,1)+P(m,1)Q(m,0)\\
C(m,2) &= P(m,0)Q(m,2)+P(m,1)Q(m,1)+P(m,2)Q(m,0)\\
&\vdots\\
C(m,m) &= P(m,0)Q(m,m)+P(m,1)Q(m,m-1)+\cdots+P(m,m)Q(m,0)\\
C(m,m+1) &= P(m,0)Q(m,m+1)+P(m,1)Q(m,m)+\cdots+P(m,m+1)Q(m,0)\\
&\vdots\\
C(m,m+n) &= P(m,0)Q(m,m+n)+P(m,1)Q(m,m+n-1)+\cdots+P(m,m+1)Q(m,n-1)\\
&\vdots
\end{aligned}
$$

index k, which can be easily proved or verified numerically. As shown in Fig. 2, for a fixed m, $C(m,k)$ decreases quickly with the increase of k; moreover, the larger m is, the faster $C(m,k)$ decreases as k increases. Note that when $k \geq 2$, the values of $C(m,k)$ become negligible and $\rho^k(s,t)$ also becomes smaller; hence, from (17), the auto-correlation function of a correlated Nakagami-m fading channel can be approximated by

$$
\begin{aligned}
R(s,t) &\approx \frac{\pi\sqrt{\eta_s\eta_t}}{4}\left[\frac{(2m-1)!!}{(2m-2)!!}\right]^2\cdot[C(m,0)\\
&\qquad + C(m,1)\rho(s,t)]\\
&\overset{(a)}{=} \frac{\pi\sqrt{\eta_s\eta_t}}{4}\left[\frac{(2m-1)!!}{(2m-2)!!}\right]^2(1+C(m,1)\rho(s,t)),
\end{aligned}
\tag{20}
$$

where (a) is because $C(m,0)=1$ for all m.

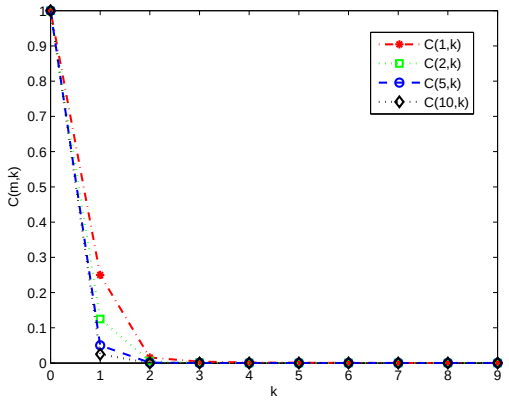

Fig. 2. $C(m,k)$ is a positive and dramatically decreasing series as k increases, for any positive integer m

For a correlated Rayleigh fading channel, i.e., Nakagami-m fading channel with $m=1$, we have the following corollary.

Corollary 1 *The auto-correlation function $R(s,t)$ of a correlated Rayleigh fading process $X(t)$ is given by*

$$
R(s,t) = \frac{\pi}{4}\sqrt{\eta_s\eta_t}(1-\rho(s,t))^2\cdot {}_2F_1\left(\frac{3}{2},\frac{3}{2};1;\rho(s,t)\right).
\tag{21}
$$

(21) can be obtained by plugging $m=1$ in (16).

Similarly, using the expression of ${}_2F_1(\frac{3}{2},\frac{3}{2};1;\rho(s,t))$ and using the Taylor series expansion of $(1-\rho)^2$, we can simplify (21) and obtain

$$
\begin{aligned}
R(s,t) =& \frac{\pi}{4}\sqrt{\eta_s\eta_t}(1-\rho(s,t))^2\\
&\cdot\sum_{k=0}^{\infty}\left[\frac{(2k+1)!!}{(2k)!!}\right]^2\rho^k(s,t)\\
=& \frac{\pi}{4}\sqrt{\eta_s\eta_t}\sum_{k=0}^{\infty}A(k)\rho^k(s,t),
\end{aligned}
\tag{22}
$$

where $A(k)=B(k)-2B(k-1)+B(k-2)$, in which $B(n)=[\frac{(2n+1)!!}{(2n)!!}]^2$ and $B(-2)=B(-1)=0$.

Furthermore, if $|\rho(s,t)|<1$, then $\lim_{k\to\infty}A(k)\rho^k(s,t)=0$. This can be easily proved or verified numerically by the fact that $A(k)$ is a positive and dramatically decreasing sequence. As shown in Fig. 2, $C(1,k)=A(k)$ decreases quickly with k. For example, $A(0)=C(1,0)=1, A(1)=C(1,1)=0.25, A(2)=C(1,2)=0.0156,\cdots$. Note that when $k\geq 2$, the values of $A(k)$ become negligible and meanwhile, $\rho^k(s,t)$ also becomes smaller; hence, from (22), the auto-correlation function of a Rayleigh fading channel can be approximated by

$$
R(s,t) \approx \frac{\pi}{4}\sqrt{\eta_s\eta_t}(A(0)+A(1)\rho(s,t)).
\tag{23}
$$

DOI: 10.1002/wcm

It is known that $R(s,t) = Cov(s,t) + \mu_s\mu_t$, where $Cov(s,t)$ is the covariance between $X(s)$ and $X(t)$, and $\mu_t = E[X(t)]$. Hence, non-stationary $R(s,t)$ can be decomposed into non-stationary second moment and non-stationary first moment. The expectation μ_t of a Nakagami-m fading process is given by

$$\begin{aligned}\mu_t =& \int_0^\infty x \cdot \frac{2}{\Gamma(m)\eta_t^m} x^{2m-1} e^{-x^2/\eta_t} \cdot dx \\ =& \frac{\sqrt{\pi\eta_t}}{2} \frac{(2m-1)!!}{(2m-2)!!},\end{aligned} \tag{24}$$

where $\eta_t = E[X^2(t)]/m$. Then we have

$$\begin{aligned} Cov(s,t) &= R(s,t) - \mu_s\mu_t \\ &\overset{(a)}{=} \frac{\pi\sqrt{\eta_s\eta_t}}{4}\left[\frac{(2m-1)!!}{(2m-2)!!}\right]^2 \\ &\quad \cdot \sum_{k=1}^{\infty} C(m,k)\rho^k(s,t) \qquad (25) \\ &\overset{(b)}{\approx} \frac{\pi\sqrt{\eta_s\eta_t}}{4}\left[\frac{(2m-1)!!}{(2m-2)!!}\right]^2 \\ &\quad C(m,1)\cdot\rho(s,t), \qquad (26)\end{aligned}$$

where (a) is due to (17) and (24); (b) is due to the approximation of $R(s,t)$ in (20). Hence, $Cov(s,t)$ is determined by η_s, η_t, and $\rho(s,t)$.

Similarly, for the Nakagami-m fading with $m = 1$, i.e., Rayleigh fading, we have

$$\begin{aligned} Cov(s,t) &\overset{(a)}{=} \frac{\pi}{4}\sqrt{\eta_s\eta_t}\sum_{k=1}^{\infty} A(k)\rho^k(s,t) \\ &\overset{(b)}{\approx} \frac{\pi\sqrt{\eta_s\eta_t}}{4} A(1)\cdot\rho(s,t), \qquad (27)\end{aligned}$$

where (a) is due to (22) and (24); (b) is due to the approximation of $R(s,t)$ in (23).

From the ES theory, $Cov(s,t)$ can be represented by

$$\begin{aligned} Cov(s,t) &= \int_{-\infty}^{+\infty} \widetilde{A}_s^*(\omega)\widetilde{A}_t(\omega)e^{j\omega(s-t)}d\widetilde{\mu}(\omega) \\ &= \int_{-\infty}^{+\infty} \widetilde{A}_s^*(\omega)\widetilde{A}_t(\omega)e^{j\omega(s-t)}\widetilde{h}(\omega)d\omega, \end{aligned} \tag{28}$$

where the measure $\widetilde{\mu}(\omega)$ is absolutely continuous and $\widetilde{h}(\omega)$ is the corresponding *evolutionary spectral density* function, i.e., $d\widetilde{\mu}(\omega) = \widetilde{h}(\omega)d\omega$. Note that we use $\widetilde{A}_t(\omega)$ and $\widetilde{h}(\omega)$ instead of $A_t(\omega)$ and $h(\omega)$ to distinguish $Cov(s,t)$ from $R(s,t)$.

4.2. Non-stationary Nakagami-m Fading Channel Simulator

Algorithm 2 shows an ES-based channel simulator that generates a non-stationary Nakagami-m fading process, given user-specified η_t and $\rho(s,t)$.

Algorithm 2 *Non-stationary Nakagami-m fading channel simulator.*

1. ***Input***: η_t $(\forall t)$ and $\rho(s,t)$ $(\forall s, \forall t)$
2. *Given η_s, η_t, and $\rho(s,t)$, compute $Cov(s,t)$ via (25).*
3. *Decompose $Cov(s,t)$ and obtain $\widetilde{A}_t(\omega)$ and $\widetilde{h}(\omega)$ that satisfy (28).*
4. *Compute the inverse Fourier transform of $\widetilde{A}_t(\omega)$, i.e., (12), and obtain $k_t(u)$.*
5. *Given $\widetilde{h}(\omega)$ and $k_t(u)$, generate $X(t)$ via the system shown in Fig. 1(b).*
6. $Y(t) = X(t) + \frac{\sqrt{\pi\eta_t}}{2}\frac{(2m-1)!!}{(2m-2)!!}$.
7. ***Output***: $Y(t)$.

Next, we show an example for Algorithm 2.

In this example, the input for Algorithm 2 is given as below.

- η_t can be any bounded deterministic function of time t and $\eta_t > 0$ $(\forall t)$.
- $\rho(s,t)$ is given by

$$\begin{aligned}\rho(s,t) =& \sqrt{\frac{2(|t|+\varepsilon)(|s|+\varepsilon)}{(|t|+\varepsilon)^2+(|s|+\varepsilon)^2}} \\ & \cdot e^{-\frac{(s-t)^2}{4((|s|+\varepsilon)^2+(|t|+\varepsilon)^2)}},\end{aligned} \tag{29}$$

  where ε can be any positive real number.

There are five reasons why we choose the form of $\rho(s,t)$ given in (29). First, it has a simple form (i.e., Gaussian form). Second, $\rho(s,t) = \rho(t,s)$. Third, according to (17), the resulting auto-correlation function $R(s,t)$ cannot be simplified to a function of $|s-t|$. Fourth, the given $\rho(s,t)$ satisfies $|\rho(s,t)| \le 1$, which can be easily proved. Fifth, the given $\rho(s,t)$ satisfies the properties that 1) for fixed s, $\rho(s,t)$ reduces as $|s-t|$ increases, and 2) $\rho(s,t)$ reaches its maximum value only when $s = t$.

Next, we show a decomposition of $Cov(s,t)$, for $\rho(s,t)$ given in (29).

Proposition 2 *Given $\rho(s,t)$ in (29), its corresponding $Cov(s,t)$ can be represented by (28), where*

$$\widetilde{A}_t(\omega) = \sqrt{\eta_t\cdot(|t|+\varepsilon)}e^{-\omega^2(|t|+\varepsilon)^2}, \tag{30}$$

DOI: 10.1002/wcm

$$\widetilde{h}(\omega) = \frac{\sqrt{2\pi}C(m,1)}{4}[\frac{(2m-1)!!}{(2m-2)!!}]^2. \quad (31)$$

In other words, $\widetilde{A}_t(\omega)$ in (30) and $\widetilde{h}(\omega)$ in (31) satisfy (28), for $\rho(s,t)$ given in (29).

Proposition 2 is proved in Appendix .2. Obviously, $\widetilde{h}(\omega)$ in (31) is a constant. Moreover, $k_t(u)$ is given by

$$\begin{aligned} k_t(u) &= \int_{-\infty}^{+\infty} \widetilde{A}_t(\omega) e^{j\omega u} d\omega \\ &= \frac{\sqrt{\eta_t \pi}}{(|t|+\varepsilon)^{\frac{3}{2}}} e^{-\frac{u^2}{4(|t|+\varepsilon)^2}}. \end{aligned} \quad (32)$$

Now, we can run Step 5 and Step 6 of Algorithm 2, and output non-stationary Nakagami-m fading process $Y(t)$.

4.3. Stationary Nakagami-m Fading Channel Simulator

In this section, we show an example that illustrates Algorithm 2 can also generate a stationary Nakagami-m fading process, i.e., a stationary channel model is a special case for our ES-based non-stationary channel model.

In this example, the input for Algorithm 2 is given as below.

- $\eta_t = \eta$ $(\forall t)$, where $\eta > 0$ is a constant.
- $\rho(s,t)$ is given by

$$\rho(s,t) = e^{-|s-t|}. \quad (33)$$

According to (33), (26), (28), and the following equality

$$\frac{1}{2\pi}\int_{-\infty}^{+\infty} \frac{2}{1+\omega^2} e^{j\omega|\tau|} d\omega = e^{-|\tau|}, \quad (34)$$

we obtain the following $\widetilde{A}_t(\omega)$ and $\widetilde{h}(\omega)$ that satisfy (28):

$$\widetilde{h}(\omega) = \frac{\pi\eta C(m,1)}{2(1+\omega^2)}[\frac{(2m-1)!!}{(2m-2)!!}]^2, \quad (35)$$

$$\widetilde{A}_t(\omega) = 1. \quad (36)$$

Then, $k_t(u)$ is given by

$$k_t(u) = \int_{-\infty}^{+\infty} \widetilde{A}_t(\omega) e^{j\omega u} d\omega = \delta(u). \quad (37)$$

Now, we can run Step 5 and Step 6 of Algorithm 2, and output stationary Nakagami-m fading process $Y(t)$. Obviously, if the simulator is to generate a stationary fading process, Part (ii) in Fig. 1(b) is not needed and can be removed.

4.4. Trace-Driven Non-stationary Nakagami-m Fading Channel Simulator

In this section, we present a trace-driven non-stationary channel simulator. Since we only know one analytically tractable ES-based channel model (presented in Section 4.2), the trace-driven non-stationary channel simulator shown in Algorithm 3 will use the non-stationary Nakagami-m fading process in Section 4.2 as a reference model. In the future, if more analytically tractable ES-based channel models are identified, we will use Bayesian Information Criterion (BIC) or Minimum Description Length (MDL) criterion to choose a channel model that matches the statistics of the given trace of channel gains.

Algorithm 3 *Trace-driven non-stationary Nakagami-m fading channel simulator.*

1. ***Input**: a measured channel gain sequence $x(t)$ $(t = 1, \cdots, N_x)$; N_s, which is odd.*
2. *Use a maximum likelihood estimator [18] or a moment-based estimator [19][20] to estimate m of Nakagami-m distribution, which matches the marginal distribution of $x(t)$.*
3. *Estimate η_t via (42).*
4. *Estimate $\rho(s,t)$ via (44).*
5. *Estimate ε by solving $\min_\varepsilon ||\rho_r(s,t) - \rho(s,t)||_2$, where $||\cdot||_2$ is 2-norm in $\mathcal{L}^2$ space, $\rho_r(s,t)$ is given by (29), and $\rho(s,t)$ is given by (44).*
6. *Given m, compute $\widetilde{h}(\omega)$ via (31).*
7. *Given η_t and ε, compute $k_t(u)$ via (32).*
8. *Given $\widetilde{h}(\omega)$ and $k_t(u)$, generate $X(t)$ via the system shown in Fig. 1(b).*
9. $Y(t) = X(t) + \frac{\sqrt{\pi\eta_t}}{2}\frac{(2m-1)!!}{(2m-2)!!}$.
10. ***Output**: $Y(t)$.*

Given $x(t)$ and N_s, we estimate η_t and $\rho(s,t)$, for $s,t = (N_s-1)/2+1, \cdots, N_x-(N_s-1)/2$, by the

DOI: 10.1002/wcm

following equations:

$$\widehat{\mu}_{X_t} = \frac{1}{N_s}\sum_{k=t-\frac{N_s-1}{2}}^{t+\frac{N_s-1}{2}} x(k), \quad (38)$$

$$\widehat{\nu}^2_{X_t} = \frac{\sum_{k=t-\frac{N_s-1}{2}}^{t+\frac{N_s-1}{2}}(x(k)-\widehat{\mu}_{X_t})^2}{N_s-1}, \quad (39)$$

$$\widehat{\mu}_{X_t^2} = \widehat{\nu}^2_{X_t}+\widehat{\mu}^2_{X_t}, \quad (40)$$

$$\widehat{\nu}^2_{X_t^2} = \frac{\sum_{k=t-\frac{N_s-1}{2}}^{t+\frac{N_s-1}{2}}(x^2(k)-\widehat{\mu}_{X_t^2})^2}{N_s-1}, \quad (41)$$

$$\widehat{\eta}_t = \frac{\widehat{\mu}_{X_t^2}}{m}, \quad (42)$$

$$\widehat{Cov}(s,t) = \frac{1}{N_s}\sum_{k=-\frac{N_s-1}{2}}^{\frac{N_s-1}{2}} x^2(s+k)x^2(t+k) - \widehat{\mu}_{X_s^2}\cdot\widehat{\mu}_{X_t^2}, \quad (43)$$

$$\widehat{\rho}(s,t) = \frac{\widehat{Cov}(s,t)}{\sqrt{\widehat{\nu}^2_{X_s^2}\cdot\widehat{\nu}^2_{X_t^2}}}. \quad (44)$$

Now, we discuss how to choose the value of N_s. First, we assume that the sampling interval Δt for measuring the channel gain $x(t)$ is sufficiently small so that for the time period that contains a large number of samples, i.e., N_s samples of $x(t)$, the channel gain process $x(t)$ can be regarded as relatively stationary.

5. Simulation Results

In this section, we conduct simulations to study the accuracy of our ES-based channel model. This section is organized as below. Section 5.1 presents an algorithm for estimating the evolutionary spectrum of a stochastic process, which is summarized in Ref. [9] and originally proposed in Ref. [21]. Section 5.2 shows simulation results.

5.1. Algorithm for Estimating ES

Suppose that a general process $X(t)$ has an expression of the form (9) and consider a more general linear transform below.

$$Y(t) = \int_{-\infty}^{+\infty} g(u)X(t-u)e^{j\omega_0(t-u)}du, \quad (45)$$

where $\omega_0 \in \mathbb{R}$ is an arbitrary frequency. Replacing $X(t)$ by (9), we have

$$Y(t) = \int_{-\infty}^{+\infty} G_{t,\omega+\omega_0}(\omega)A_t(\omega+\omega_0)e^{j\omega t}d\mathcal{Z}(\omega+\omega_0), \quad (46)$$

$$E[|Y(t)|^2] = \int_{-\infty}^{+\infty}|G_{t,\omega+\omega_0}(\omega)|^2|A_t(\omega+\omega_0)|^2 \cdot d\mu(\omega+\omega_0), \quad (47)$$

where, for any t, λ, θ,

$$G_{t,\lambda}(\theta) = \int_{-\infty}^{+\infty} g(u)\frac{A_{t-u}(\lambda)}{A_t(\lambda)}e^{-j\theta u}du. \quad (48)$$

It can be seen that the function $G_{t,\lambda}(\theta)$ is approximately equal to the Fourier transform of $g(u)$, denoted by $G(\theta)$, if, for any λ, the value of $\frac{A_{t-u}(\lambda)}{A_t(\lambda)}$ is close to 1, which means that $A_{t-u}(\lambda)$ is slowly time varying compared with the function $g(u)$ as time lapse u increases. Thus, we assume that $g(u)$ decays rapidly to zero as $|u|\to\infty$ and that $A_{t-u}(\lambda)$ is approximately constant over the range of u for which $g(u)$ is not very close to zero. In this case, we consider that $G_{t,\lambda}(\theta)\approx G(\theta)$ holds for any t, λ and θ. Then, we may write

$$d\mathcal{H}_t^Y(\omega) \approx |G(\omega)|^2 d\mathcal{H}_t^X(\omega+\omega_0), \quad (49)$$

where $d\mathcal{H}_t^X(\omega+\omega_0) = |A_t(\omega+\omega_0)|^2 d\mu(\omega+\omega_0)$, according to the definition of evolutionary spectrum (11). The formula (49) provides the basis for the algorithm of estimating the evolutionary spectrum of the process $X(t)$. The details is given as below.

First, to define a slowly time varying function whose Fourier transform must be highly concentrated in the region of zero frequency, a new variable $B_{\mathcal{F}}$ is introduced for a family of functions $\mathcal{F}\equiv\{A_t(\omega)e^{j\omega t}\}$ to characterize its slowly time varying degree. That is,

$$B_{\mathcal{F}} = [\sup_{\omega}\{B_{\mathcal{F}}(\omega)\}]^{-1}; B_{\mathcal{F}}(\omega) = \int_{-\infty}^{+\infty}|\theta||d\mathcal{K}_\omega(\theta)|, \quad (50)$$

where $B_{\mathcal{F}}(\omega)$ is a measure of "width" of the spectrum of $A_t(\omega)$. For a fixed ω, the reciprocal of $B_{\mathcal{F}}(\omega)$ describes the slowly time varying degree of $A_t(\omega)$. Thus, the physical meaning of $B_{\mathcal{F}}$ is the minimum time interval during which, for all ω, $A_t(\omega)$ can be considered slowly time varying.

Next, to measure the "width" of a sharply decreasing filter $g(u)$, another parameter B_g is defined by

$$B_g = \int_{-\infty}^{+\infty}|u||g(u)|du. \quad (51)$$

Moreover, suppose that the filter $g(u)$ is square integrable and normalized, so that

$$2\pi\int_{-\infty}^{+\infty}|g(u)|^2du = \int_{-\infty}^{+\infty}|G(\omega)|^2d\omega = 1. \quad (52)$$

DOI: 10.1002/wcm

Now, we consider the case that if the filter $g(u)$ and the family of oscillatory functions $\mathcal{F}$ satisfies

$$B_g \ll B_{\mathcal{F}}. \tag{53}$$

Then, according to Eq. (47) to Eq. (49), we may write

$$\begin{aligned} E[|Y(t)|^2] &\approx \int_{-\infty}^{+\infty} |G(\omega)|^2 d\mathcal{H}_t^X(\omega+\omega_0) \\ &= \int_{-\infty}^{+\infty} |G(\omega)|^2 h_t^X(\omega+\omega_0) d\omega. \end{aligned} \tag{54}$$

Furthermore, if $|G(\omega)|^2$ in (52) is sharply decreasing as $|\omega|$ increases, then $|G(\omega)|^2$ is approximately equal to the δ-function of ω. Combining this with (53) and (54), we have

$$h_t^e(\omega_0) \approx E[|Y(t)|^2], \tag{55}$$

where $h_t^e(\omega_0)$ denotes the estimated evolutional spectrum of $X(t)$ at frequency ω_0.

The following summarizes the algorithm for estimating the ES of $X(t)$.

1. Choose a sharply decreasing filter $g(u)$ satisfying (52) and (53).
2. Take the following linear transform of samples of $X(t)$ in time interval $[t-T, t]$ for each ω_0,

$$\hat{Y}(t) = \int_{t-T}^{t} g(u)\hat{X}(t-u)e^{j\omega_0(t-u)}du, \tag{56}$$

where $\hat{X}(t)$ denotes the realization/sample of $X(t)$. Eq. (56) is for continuous time t. For discrete time, we have

$$\hat{Y}(n) = \Sigma_{n=0}^{N} g_n \hat{X}_{N-n} e^{j\omega_0(N-n)}du. \tag{57}$$

3. Compute the time average of $\hat{Y}(t)$ in time interval $[t-T, t]$ for each ω_0, which is the estimate $h_t^e(\omega_0)$ due to (55).

5.2. Simulation Results

In this section, we show simulation results to verify whether our ES-based channel model is able to produce a channel gain process whose evolutionary spectrum matches user-specified ES. The section is organized as below. Section 5.2.1 demonstrates the generality of our ES based model by showing that it can also be used to generate stationary channel gain processes with good accuracy in terms of user-specified ES. In Section 5.2.2, we use our ES based model to generate a non-stationary channel gain process and study its accuracy. Section 5.2.3 shows the accuracy of Algorithm 2 in simulating a non-stationary channel gain process under a mobility pattern. In Section 5.2.4, we present the results of our trace-driven channel simulator, i.e., Algorithm 3.

5.2.1. *Accuracy of Algorithm 2 in Simulating a Stationary Channel Gain Process*

In this section, we use Algorithm 2 to generate a stationary channel gain process, given user-specified ES, and study the accuracy of Algorithm 2.

For a stationary channel gain process, we have $\rho(s,t) = e^{-|s-t|}$. Since $A_t(\omega) \equiv 1$, the linear time-varying filter in the channel simulator in Fig. 1(b) can be removed. We assume $\eta_t = 1$ $(\forall t)$ and the sampling interval is 1ms. We use the Rice model [22, 23, 24] with the number of branches $N = 20$ to implement the linear time-invariant filter in Fig. 1(b) and generate a stationary channel gain process whose psd is given by $h(\omega) = \frac{\pi\eta C(m,1)}{2(1+\omega^2)}[\frac{(2m-1)!!}{(2m-2)!!}]^2$. Since the ES of a stationary process reduces to the power spectral density (psd) of the process, we can use the classical spectral estimation algorithm, e.g., Burg spectral estimation method, to estimate the psd of the stationary channel gain process generated by Algorithm 2.

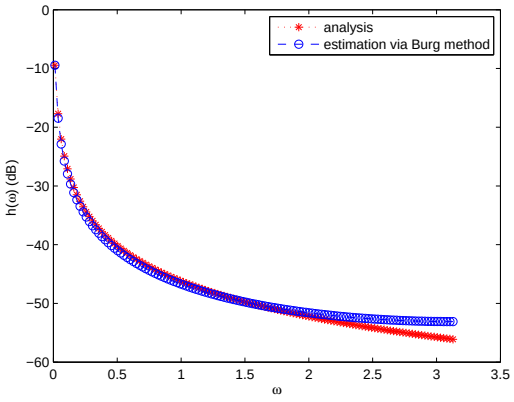

Fig. 3. Power spectral density of a stationary channel gain process

Fig. 3 shows 1) user-specified psd $h(\omega) = \frac{\pi\eta C(m,1)}{2(1+\omega^2)}[\frac{(2m-1)!!}{(2m-2)!!}]^2$, labeled as 'analysis', and 2) the estimated psf of the channel gain process generated by Algorithm 2 via Burg method, labeled as 'estimation via Burg method'. It is observed that the psd obtained by Burg method agrees well with the user-specified

DOI: 10.1002/wcm

psd. This indicates high degree of accuracy of Algorithm 2 in simulating a stationary channel gain process.

5.2.2. Accuracy of Algorithm 2 in Simulating a Non-stationary Channel Gain Process

In this section, we use Algorithm 2 to generate a non-stationary channel gain process, given user-specified ES, and study its accuracy.

For a non-stationary channel gain process, we let $\rho(s,t) = \sqrt{\frac{2(|t|+\varepsilon)(|s|+\varepsilon)}{(|t|+\varepsilon)^2+(|s|+\varepsilon)^2}} e^{-\frac{(s-t)^2}{4((|s|+\varepsilon)^2+(|t|+\varepsilon)^2)}}$. We set the carrier frequency to $2GHz$ and the Doppler frequency spread to 30Hz. In the simulation, we choose

$$g(u) = \begin{cases} \dfrac{1}{2\sqrt{h\pi}}, & |u| \le h, \qquad (58a) \\ 0, & |u| > h. \qquad (58b) \end{cases}$$

Then $|G(\omega)|^2 = \frac{1}{\pi}\frac{\sin^2(h\omega)}{h\omega^2}$. We let $h = 7$. Moreover, according to (51), we can find that the filter width corresponding to $g(u)$ of the above form is given by

$$B_g = 7^{3/2}/(2\sqrt{\pi})$$

and for the family $\mathcal{F}$ given by (30), according to (50), after simplification, we have

$$B_{\mathcal{F}}(\omega) \approx 2\sqrt{\pi}\varepsilon\omega^{\frac{3}{2}}$$

and then

$$B_{\mathcal{F}} = [\sup_{\omega}\{B_{\mathcal{F}}(\omega)\}]^{-1} \approx \varepsilon^{-1}/(2\sqrt{\pi}\omega_m^{\frac{3}{2}})$$

For a sufficiently small ε and finite Doppler spread, i.e., $\omega_m < \infty$, the algorithm for estimating ES is accurate. We let $\varepsilon = 10^{-5}$ and $\omega_m = 30$Hz in the simulation. Thus, we have $B_g/B_{\mathcal{F}} \approx 0.03$.

We first examine the ES at $t = 50ms$ for Nakagami-m fading with $m = 1$. Fig. 4(a) shows user-specified ES $d\mathcal{H}_t(\omega) = |\widetilde{A}_t(\omega)|^2\widetilde{h}(\omega)$, where $\widetilde{A}_t(\omega)$ is given by (30) and $\widetilde{h}(\omega)$ is given by (31). Fig. 4(b) shows the estimated ES of the non-stationary channel gain process generated by Algorithm 2 for the given user-specified ES; the estimated ES is obtained by the estimation method in Section 5.1. It is observed that the estimated ES agrees well with the user-specified ES.

We then examine the ES at $t = 100ms$ for Nakagami-m fading with $m = 2$. Fig. 5(a) shows user-specified ES $d\mathcal{H}_t(\omega) = |\widetilde{A}_t(\omega)|^2\widetilde{h}(\omega)$, where $\widetilde{A}_t(\omega)$ is given by (30) and $\widetilde{h}(\omega)$ is given by (31). Fig. 5(b) shows the estimated ES of the non-stationary channel gain process generated by Algorithm 2 for the given user-specified ES. We again observe that the estimated ES agrees well with the user-specified ES. This indicates high degree of accuracy of Algorithm 2 in simulating a non-stationary channel gain process.

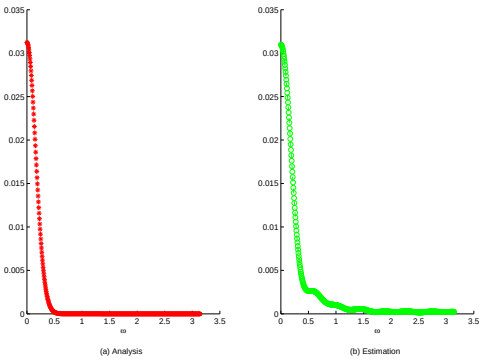

Fig. 4. Analytical and estimated evolutionary spectrum for a non-stationary process at $t = 50ms$ $(m = 1)$

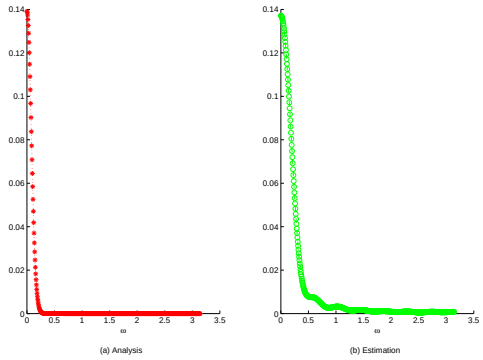

Fig. 5. Analytical and estimated evolutionary spectrum for a non-stationary process at $t = 100ms$ $(m = 2)$

5.2.3. Accuracy of Algorithm 2 in Simulating a Non-stationary Channel Gain Process under a Mobility Pattern

In this section, we use Algorithm 2 to generate a non-stationary channel gain process, for a given mobility pattern, and study its accuracy.

We consider a mobility pattern shown in Fig. 6. First, the vehicle accelerates with acceleration of $2.682m/s^2$ till its speed reaches 60 miles per hour (mph). This takes about 10 seconds. Then, the vehicle keeps the speed of 60 mph for 20 seconds. Finally,

DOI: 10.1002/wcm

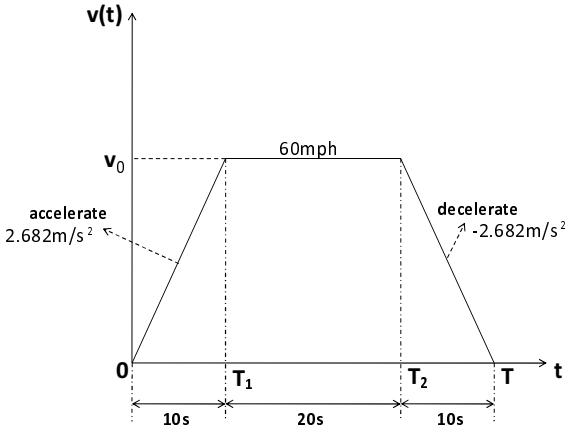

Fig. 6. Mobility pattern

the acceleration becomes $-2.682m/s^2$ and it takes 10 seconds for the vehicle to stop.

The maximum Doppler frequency f_m can be computed by

$$f_m = f_c \cdot \frac{\upsilon}{c} \cos\theta \tag{59}$$

where υ is the velocity of the vehicle, c is the speed of light, θ is the angle between the moving direction and the signal receiving direction and f_c is the carrier frequency. In the simulation, we let $f_c = 2GHz$ and $\theta = 30°$. From (59), we have $f_m = 154.87Hz$ for $\upsilon = 60$ mph.

The Gans' Doppler spectrum $S_{E_z}(f)$ is given by [1]

$$S_{E_z}(f) = \frac{1.5}{\pi f_m \sqrt{1-((f-f_c)/f_m)^2}}, \quad f \in [f_c - f_m, f_c + f_m]. \tag{60}$$

As shown in Fig. 6, the velocity υ is time varying. Hence, from (59), the Doppler frequency is also time varying; we denote it by $f_m(t)$. Consequently, the Gans' Doppler spectrum is also time varying. We denote it by $S_{E_z,t}(\omega)$, where $\omega = 2\pi f$, and write

$$S_{E_z,t}(\omega) = \frac{3}{\omega_m(t)\sqrt{1-((\omega-\omega_c)/\omega_m(t))^2}}, \quad \omega \in [\omega_c - \omega_m, \omega_c + \omega_m]. \tag{61}$$

According to the definition of evolutionary spectrum, we have

$$A_t(\omega) = \sqrt{S_{E_z,t}(\omega)} = \frac{\sqrt{3}}{\sqrt{\omega_m(t)\sqrt{1-((\omega-\omega_c)/\omega_m(t))^2}}}, \quad \omega \in [\omega_c - \omega_m(t), \omega_c + \omega_m(t)], \tag{62}$$

under the condition that $h(\omega) = 1$. Then, $k_t(u)$ is given by

$$\begin{aligned}
k_t(u) &= \int_{-\infty}^{+\infty} A_t(\omega) e^{j\omega u} d\omega \\
&= \int_{-\infty}^{+\infty} \sqrt{S_{E_z,t}(\omega)} e^{j\omega u} d\omega \\
&= \int_{\omega_c-\omega_m(t)}^{\omega_c+\omega_m(t)} \frac{\sqrt{3} e^{j\omega u} d\omega}{2\sqrt{\omega_m(t)\sqrt{1-((\omega-\omega_c)/\omega_m(t))^2}}} + \\
&\quad \int_{-\omega_c-\omega_m(t)}^{-\omega_c+\omega_m(t)} \frac{\sqrt{3} e^{j\omega u} d\omega}{2\sqrt{\omega_m(t)\sqrt{1-((-\omega+\omega_c)/\omega_m(t))^2}}} \\
&= \frac{\sqrt{3}}{2} \{ \int_{\omega_c-\omega_m(t)}^{\omega_c+\omega_m(t)} [\omega_m^2(t) - (\omega-\omega_c)^2]^{-\frac{1}{4}} e^{j\omega u} d\omega + \\
&\quad \int_{-\omega_c-\omega_m(t)}^{-\omega_c+\omega_m(t)} [\omega_m^2(t) - (-\omega+\omega_c)^2]^{-\frac{1}{4}} e^{j\omega u} d\omega \} \\
&\overset{(a)}{=} \cos(\omega_c u) \int_{-\omega_m(t)}^{+\omega_m(t)} (\omega_m^2(t) - x^2)^{-\frac{1}{4}} e^{jxu} dx \\
&\overset{(b)}{=} \cos(\omega_c u) \int_{-1}^{+1} \sqrt{\omega_m(t)} (1-t^2)^{-\frac{1}{4}} e^{j\omega_m(t)\cdot ut} dt \\
&\overset{(c)}{=} \sqrt{\pi}\Gamma(\frac{3}{4}) (\frac{2\omega_m(t)}{u})^{\frac{1}{4}} J_{\frac{1}{4}}(\omega_m(t)\cdot u)\cos(\omega_c u),
\end{aligned} \tag{63}$$

where (a) is due to replacing $(\omega - \omega_c)$ by x; (b) is due to replacing x by $t \times \omega_m(t)$; (c) is due to the use of the following integral,

$$\int_{-1}^{1} (1-t^2)^{\nu-\frac{1}{2}} e^{jzt} \mathbf{d}t = \frac{\sqrt{\pi}\Gamma(\nu+1/2)}{(z/2)^\nu} J_\nu(z), \quad \mathrm{Re}(\nu) > -\frac{1}{2}, \tag{64}$$

where $\Gamma(\cdot)$ is the Gamma function and $J_\nu(\cdot)$ is the ν-th order Bessel function of the first kind and we let $\nu = \frac{1}{4}$ and $z = \omega_m(t)\cdot u$.

We first examine the ES at $t = 3s$ where Doppler frequency $f_m = 46.45Hz$ according to the velocity in Fig. 6 and (59). Fig. 7 shows user-specified ES $d\mathcal{H}_t(\omega) = |A_t(\omega)|^2 h(\omega)$, where $A_t(\omega)$ is given by (62) and $h(\omega) = 1$, compared with the estimated ES of the non-stationary channel gain process generated by Algorithm 2 for the given user-specified ES; the estimated ES is obtained by the estimation method in Section 5.1. It is observed that the estimated ES agrees well with the user-specified ES.

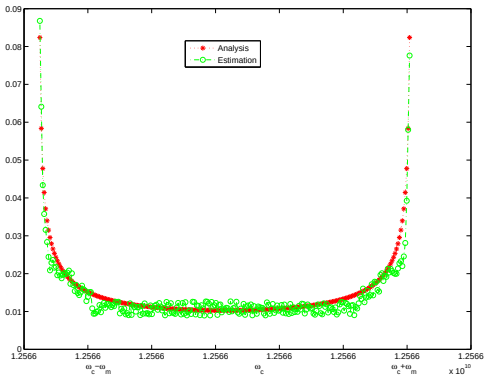

Fig. 7. Analytical and estimated evolutionary spectrum at $t = 3s$ with Doppler frequency $46.45Hz$

We then examine the ES at $t = 33s$ where Doppler frequency $f_m = 108.39Hz$ according to the velocity in Fig. 6. Fig. 8 shows user-specified ES $d\mathcal{H}_t(\omega) = |A_t(\omega)|^2 h(\omega)$, where $A_t(\omega)$ is given by (62) and $h(\omega) = 1$, compared with the estimated ES of the non-stationary channel gain process generated by Algorithm 2 for the given user-specified ES. We again observe that the estimated ES agrees well with the user-specified ES. Hence, Algorithm 2 is able to accurately simulate a non-stationary channel gain process according to the user-specified mobility pattern.

5.2.4. *Accuracy of Algorithm 3*

In this section, we use Algorithm 3 to generate a non-stationary channel gain process whose ES matches the ES of a given channel gain trace, and study its accuracy.

The two channel gain traces used in this section, were collected on a moving vehicle, which was moving at a time-varying speed between 50 mph and 70 mph on a highway in the San Francisco Bay Area, California. The channel gain, actually, signal-to-interference-plus-noise-ratio (SINR), was measured

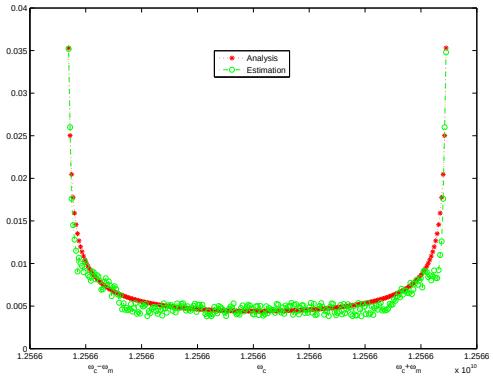

Fig. 8. Analytical and estimated evolutionary spectrum at $t = 33s$ with Doppler frequency $108.39Hz$

every $1.67ms$ for approximately one hour. The wireless system is 3G Evolution-Data Optimized (EV-DO). For Algorithm 3, we choose $N_s = 129$.

For the first trace, Step 2 of Algorithm 3 produces an estimate of 1.77 for m. Since our analysis requires that m be a positive integer, we let $m = 2$. We examine the ES at $t = 30min$. Fig. 9(a) shows the estimated ES of the non-stationary channel gain process generated by Algorithm 3; Fig. 9(b) shows the estimated ES of the channel gain trace. The estimated ES is obtained by the estimation method in Section 5.1. It is observed that the estimated ES of the non-stationary channel gain process generated by Algorithm 3 agrees well with that of the channel gain trace.

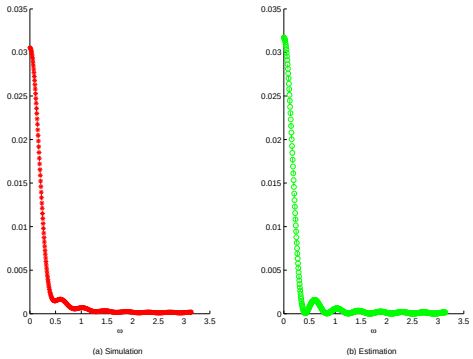

Fig. 9. Estimated evolutionary spectrum for the model-based regenerated process from simulation and original mobile-trace-1 process

For the second trace, Step 2 of Algorithm 3 produces an estimate of 1.96 for m. Since our analysis requires that m be a positive integer, we let $m = 2$. We examine the ES at $t = 30min$. Fig. 10(a)

DOI: 10.1002/wcm

shows the estimated ES of the non-stationary channel gain process generated by Algorithm 3; Fig. 10(b) shows the estimated ES of the channel gain trace. The estimated ES is obtained by the estimation method in Section 5.1. We again observe that the estimated ES of the non-stationary channel gain process generated by Algorithm 3 agrees well with that of the channel gain trace. Hence, Algorithm 3 is able to accurately simulate a non-stationary channel gain process according to the given trace of channel gain.

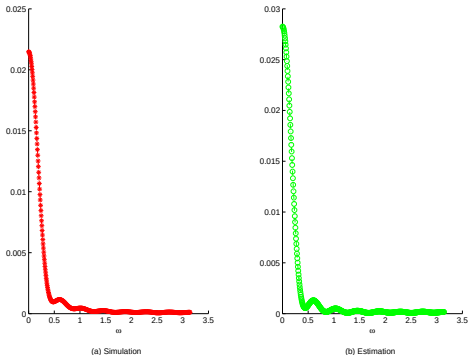

Fig. 10. Estimated evolutionary spectrum for the model-based regenerated process from simulation and original mobile-trace-2 process

6. Conclusion

In this paper, we proposed a new methodology for modeling non-stationary fading channels; we call it evolutionary-spectrum (ES) based approach. Our ES approach is capable of characterizing a general non-stationary fading channel that has an arbitrary ES (or time-varying power spectral density), indicating that it is more general than the existing piecewise-stationary models. Furthermore, our ES approach is concise. To implement our approach in practical systems, we developed Algorithm 2, i.e., an ES-based channel simulator that generates a non-stationary correlated Nakagami-m fading process, given user-specified η_t and $\rho(s,t)$. We also developed Algorithm 3, i.e., a trace-driven non-stationary channel simulator. Simulation results show that the evolutionary spectrum of the channel gain process produced by our ES-based channel model agrees well with the user-specified evolutionary spectrum or that of the trace, indicating the accuracy of our ES-based channel model in practical mobile communication systems.

Acknowledgement

We would like to thank the editor and also the reviewers for their comments which are helpful to improve our presentation. This work was supported in part by the US National Science Foundation under grant CNS-0643731, the US Office of Naval Research under grant N000140810873, NSFC/RGC Joint Research Scheme No. 60831160524, the China National Science and Technology Major Project No.2010ZX03003-003, the open research fund of National Mobile Communications Research Laboratory, Southeast University, China, NSFC No.61171064 and National Key fundamental R and D Project (973 Project) No. 2012CB316102. Dr. Dapeng Wu would like to thank Dr. Ashwin Sridharan and Sprint Advanced Technology Labs, Burlingame, CA, USA for providing the traces of channel gain measurements.

.1. Proof of Proposition 1

Proof 1 *For simplicity of notation, we replace* $X(s)$ *by* x*, replace* $X(t)$ *by* y*, and replace* $\rho(s,t)$ *by* ρ *in*

DOI: 10.1002/wcm

the derivation of $R(s,t)$.

$$
\begin{aligned}
&R(s,t)\\
=&\int_0^\infty\int_0^\infty xyf(x,y)dxdy\\
=&\int_0^\infty\int_0^\infty \frac{4(xy)^{m+1}e^{-(\eta_y x^2+\eta_x y^2)/(\eta_x\eta_y(1-\rho))}}{\Gamma(m)\eta_x\eta_y(1-\rho)(\eta_x\eta_y\rho)^{(m-1)/2}}\\
&\cdot I_{m-1}(\frac{2\sqrt{\rho}xy}{\sqrt{\eta_x\eta_y}(1-\rho)})dxdy\\
=&\int_0^\infty\int_0^\infty \frac{4(xy)^{m+1}e^{-(\eta_y x^2+\eta_x y^2)/(\eta_x\eta_y(1-\rho))}}{\Gamma(m)\eta_x\eta_y(1-\rho)(\eta_x\eta_y\rho)^{(m-1)/2}}\\
&\cdot\sum_{k=0}^\infty\frac{1}{k!\Gamma(m+k)}(\frac{\sqrt{\rho}xy}{\sqrt{\eta_x\eta_y}(1-\rho)})^{m+2k-1}dxdy\\
=&\sum_{k=0}^\infty\frac{4\cdot(\frac{\sqrt{\rho}}{\sqrt{\eta_x\eta_y}(1-\rho)})^{m+2k-1}}{\Gamma(m)\eta_x\eta_y(1-\rho)(\eta_x\eta_y\rho)^{(m-1)/2}k!\Gamma(m+k)}\\
&\cdot\int_0^\infty x^{2(m+k)}e^{-x^2/(\eta_x(1-\rho))}dx\\
&\cdot\int_0^\infty y^{2(m+k)}e^{-y^2/(\eta_y(1-\rho))}dy\\
=&\sum_{k=0}^\infty\frac{4\cdot(\frac{\sqrt{\rho}}{\sqrt{\eta_x\eta_y}(1-\rho)})^{m+2k-1}}{\Gamma(m)\eta_x\eta_y(1-\rho)(\eta_x\eta_y\rho)^{(m-1)/2}k!\Gamma(m+k)}\\
&\cdot[\eta_x(1-\rho)]^{m+k}\sqrt{\eta_x(1-\rho)\pi}\frac{[2(m+k)-1]!!}{2^{m+k+1}}\\
&\cdot[\eta_y(1-\rho)]^{m+k}\sqrt{\eta_y(1-\rho)\pi}\frac{[2(m+k)-1]!!}{2^{m+k+1}}\\
=&\sum_{k=0}^\infty\frac{\pi\{[2(m+k)-1]!!\}^2\sqrt{\eta_x\eta_y}(1-\rho)^{m+1}\rho^k}{\Gamma(m)\Gamma(m+k)k!2^{2(m+k)}}\\
=&\frac{\pi\sqrt{\eta_x\eta_y}(1-\rho)^{m+1}}{\Gamma(m)2^{m+1}}\sum_{k=0}^\infty\frac{\{[2(m+k)-1]!!\}^2\rho^k}{(2k)!![2(m+k-1)]!!}\\
=&\frac{\pi\sqrt{\eta_x\eta_y}(1-\rho)^{m+1}}{\Gamma(m)2^{m+1}}\frac{[(2m-1)!!]^2}{(2m-2)!!}\\
&\cdot{}_2F_1(m+\frac{1}{2},m+\frac{1}{2};m;\rho)\\
=&\frac{\pi\sqrt{\eta_x\eta_y}(1-\rho)^{m+1}}{4}[\frac{(2m-1)!!}{(2m-2)!!}]^2\\
&\cdot{}_2F_1(m+\frac{1}{2},m+\frac{1}{2};m;\rho).
\end{aligned}
\tag{65}
$$

This completes the proof.

.2. Proof of Proposition 2

Proof 2 *According to (26), we may write*

$$
\begin{aligned}
Cov(s,t)\approx&\frac{\pi\sqrt{\eta_s\eta_t}}{4}[\frac{(2m-1)!!}{(2m-2)!!}]^2C(m,1)\rho(s,t)\\
\overset{(a)}{=}&\frac{\pi\sqrt{\eta_s\eta_t}}{4}[\frac{(2m-1)!!}{(2m-2)!!}]^2C(m,1)\\
&\cdot\sqrt{\frac{2(|t|+\varepsilon)(|s|+\varepsilon)}{(|t|+\varepsilon)^2+(|s|+\varepsilon)^2}}\\
&\cdot e^{-\frac{(s-t)^2}{4((|s|+\varepsilon)^2+(|t|+\varepsilon)^2)}},
\end{aligned}
\tag{66}
$$

where (a) is because $\rho(s,t)$ is given by (29).

On the other hand, by substituting $\widetilde{A}_t(\omega)$ in (30) and $\widetilde{h}(\omega)$ in (31) into the right hand side of (28), we obtain

$$
\begin{aligned}
&\int_{-\infty}^{+\infty}\widetilde{A}_s^*(\omega)\cdot\widetilde{A}_t(\omega)\cdot e^{j\omega(s-t)}\cdot\widetilde{h}(\omega)d\omega\\
=&\int_{-\infty}^{+\infty}\sqrt{\eta_s(|s|+\varepsilon)}e^{-\omega^2(|s|+\varepsilon)^2}\\
&\cdot\sqrt{\eta_t(|t|+\varepsilon)}e^{-\omega^2(|t|+\varepsilon)^2}\cdot e^{j\omega(s-t)}\\
&\cdot\frac{\sqrt{2\pi}C(m,1)}{4}[\frac{(2m-1)!!}{(2m-2)!!}]^2d\omega\\
=&\frac{C(m,1)\sqrt{\eta_s\eta_t}}{4}[\frac{(2m-1)!!}{(2m-2)!!}]^2\sqrt{2\pi(|t|+\varepsilon)(|s|+\varepsilon)}\\
&\cdot\int_{-\infty}^{+\infty}e^{-\omega^2[(|s|+\varepsilon)^2+(|s|+\varepsilon)^2]}\cdot e^{j\omega(s-t)}d\omega\\
\overset{(a)}{=}&\frac{C(m,1)\sqrt{\eta_s\eta_t}}{4}[\frac{(2m-1)!!}{(2m-2)!!}]^2\sqrt{2\pi(|t|+\varepsilon)(|s|+\varepsilon)}\\
&\cdot\sqrt{\frac{\pi}{(|t|+\varepsilon)^2+(|s|+\varepsilon)^2}}e^{-\frac{(s-t)^2}{4((|s|+\varepsilon)^2+(|t|+\varepsilon)^2)}}\\
=&\frac{\pi\sqrt{\eta_s\eta_t}}{4}[\frac{(2m-1)!!}{(2m-2)!!}]^2C(m,1)\\
&\cdot\sqrt{\frac{2(|t|+\varepsilon)(|s|+\varepsilon)}{(|t|+\varepsilon)^2+(|s|+\varepsilon)^2}}e^{-\frac{(s-t)^2}{4((|s|+\varepsilon)^2+(|t|+\varepsilon)^2)}},
\end{aligned}
\tag{67}
$$

where (a) is due to the following equality

$$
\int_{-\infty}^{+\infty}e^{-\omega^2a^2}\cdot e^{j\omega b}d\omega=\frac{\sqrt{\pi}}{a}e^{-b^2/(4a^2)},\ a>0,
\tag{68}
$$

with $b=s-t$ and $a=\sqrt{(|s|+\varepsilon)^2+(|t|+\varepsilon)^2}$. Obviously, the right hand side of (66) is the same as the right hand side of (67). Hence, $\widetilde{A}_t(\omega)$ in (30) and $\widetilde{h}(\omega)$ in (31) satisfy (28), for $\rho(s,t)$ given in (29). This completes the proof.

DOI: 10.1002/wcm

References

1. T. S. Rappaport, *Wireless communications: principles and practice*. Prentice Hall: New Jersey, 2002.
2. J. Parsons and K. (Firm), *The mobile radio propagation channel*. Wiley New York, 2000.
3. P. Bello, I. ADCOM, and M. Cambridge, "Characterization of randomly time-variant linear channels," *IEEE Transactions on Communications Systems*, vol. 11, no. 4, pp. 360–393, 1963.
4. K. Sostrand, "Mathematics of the time-varying channel," *Proceedings NATO Advanced Study Institute on Signal Procesing with Emphasis on Underwater Acoustics*, vol. 2, pp. 25–1, 1968.
5. G. Matz, "Doubly underspread non-WSSUS channels: Analysis and estimation of channel statistics," in *4th IEEE Workshop on Signal Processing Advances in Wireless Communications, 2003. SPAWC 2003*, 2003, pp. 190–194.
6. ——, "On non-WSSUS wireless fading channels," *IEEE Transactions on Wireless Communications*, vol. 4, no. 5, pp. 2465–2478, 2005.
7. M. Jachan and G. Matz, "Nonstationary vector AR modeling of wireless channels," in *2005 IEEE 6th Workshop on Signal Processing Advances in Wireless Communications*, 2005, pp. 625–629.
8. I. Sen, D. W. Matolak, and W. Xiong, "Wireless Channels that Exhibit "Worse Than Rayleigh" Fading: Analytical and Measurement Results," *IEEE MILCOM*, 2006.
9. M. B. Priestley, *Spectral analysis and time series*. Academic Press: London, 1981.
10. J. Karedal, F. Tufvesson, N. Czink, A. Paier, C. Dumard, T. Zemen, C. Mecklenbrauker, and A. Molisch, "A geometry-based stochastic mimo model for vehicle-to-vehicle communications," *Wireless Communications, IEEE Transactions on*, vol. 8, no. 7, pp. 3646–3657, 2009.
11. A. Paier, J. Karedal, N. Czink, C. Dumard, T. Zemen, F. Tufvesson, A. Molisch, and C. Mecklenbr "auker, "Characterization of vehicle-to-vehicle radio channels from measurements at 5.2 ghz," *Wireless personal communications*, vol. 50, no. 1, pp. 19–32, 2009.
12. E. Parzen, *Statistical inference on time series by Hilbert space methods, I*. Applied Mathematics and Statistics Laboraotry, Stanford University, 1959.
13. ——, "Mathematical considerations in the estimation of spectra," *Technometrics*, vol. 3, no. 2, pp. 167–190, 1961.
14. M. Jachan, G. Matz, and F. Hlawatsch, "Vector time-frequency AR models for nonstationary multivariate random processes," *IEEE Transactions on Signal Processing*, vol. 57, no. 12, pp. 4646–4659, 2009.
15. M. Nakagami, "The m-distribution: A general formula of intensity distribution of rapid fading, Statistical Methods in Radio Wave Propagation," *Elmsford, NY: Pergamon*, 1960.
16. C. Tan and N. Beaulieu, "Infinite series representations of the bivariate Rayleigh and Nakagami-m distributions," *IEEE Transactions on Communications*, vol. 45, no. 10, pp. 1159–1161, 1997.
17. Wikipedia, "Online available at http://en.wikipedia.org/wiki/Hypergeometric_series."
18. J. Cheng and N. Beaulieu, "Maximum-likelihood based estimation of the Nakagami m parameter," *IEEE Communications Letters*, vol. 5, no. 3, pp. 101–103, 2001.
19. A. Abdi and M. Kaveh, "Performance comparison of three different estimators for the Nakagami m parameter using Monte Carlo simulation," *IEEE communications letters*, vol. 4, no. 4, pp. 119–121, 2000.
20. Y. Chen and N. Beaulieu, "Estimation of ricean and nakagami distribution parameters using noisy samples," in *IEEE International Conference on Communications*, 2004.
21. M. B. Priestley, "Design relations for non-stationary processes," *Journal of the Royal Statistical Society. Series B (Methodological)*, pp. 228–240, 1966.
22. M. Pätzold, *Mobile fading channels*. Wiley, 2002.
23. S. Rice, "Mathematical analysis of random noise," *Bell Syst. Tech. J*, vol. 24, pp. 46–156, 1945.
24. ——, "Mathematical analysis of random noise," *Bell Syst. Tech. J*, vol. 23, no. 3, pp. 282–332, 1944.

DOI: 10.1002/wcm

Authors' Biographies

Qing Wang received the B.S. degree in the School of Information Science and Engineering from Shandong University, Jinan, China in 2006 and his Ph.D degree from the Department of Electronic Engineering, Tsinghua University, Beijing, China in 2011. He is currently an engineer of the National Computer network Emergency Response technical Team/Coordination Center of China (CNCERT/CC). From 2008 to 2009, he visited Dept. Electrical Engineering in University of Florida as a research scholar. His research interest is in the general area of information systems and networks. Specifically, he has been working on wireless sensor and ad hoc networks, the network information theory and cross layer design, etc. He received the Tsinghua University Excellent Ph.D Graduation Thesis Award and the Best Paper Award in International Wireless Communications and Mobile Computing Conference (IWCMC) 2010. He serves as a reviewer for IEEE Transactions on Communications, IEEE Transactions on Vehicular Technology and IEEE Transactions on Wireless Communications and several international conferences.

Pingyi Fan (M'04-SM'09) received the B.S and M.S. degrees from the Department of Mathematics of Hebei University in 1985 and Nankai University in 1990, respectively, received his Ph.D degree from the Department of Electronic Engineering, Tsinghua University, Beijing, China in 1994. He is a professor of department of EE of Tsinghua University currently. From Aug. 1997 to March. 1998, he visited Hong Kong University of Science and Technology as Research Associate. From May. 1998 to Oct. 1999, he visited University of Delaware, USA, as research fellow. In March. 2005, he visited NICT of Japan as visiting Professor. From June. 2005 to July. 2005, Aug. 2006 to Sept. 2010, he visited Hong Kong University of Science and Technology for many times. He was promoted to full Professor at Tsinghua University in 2002.

Dr. Fan is a senior member of IEEE and an oversea member of IEICE. He has attended to organize many international conferences including as TPC co-Chair of IEEE International Conference on Wireless Communications, Networking and Information Security (WCNIS 2010) and TPC member of IEEE ICC, Globecom, WCNC, VTC, etc. He has served as an editor of IEEE Transactions on Wireless Communications, Inderscience International Journal of Ad Hoc and Ubiquitous Computing and Wiley Journal of Wireless Communication and Mobile Computing. He is also a reviewer of more than 14 international Journals including 10 IEEE Journals and 3 EURASIP Journals. He has received some academic awards, including the IEEE WCNC'08 Best Paper Award, ACM IWCMC'10 Best Paper Award and IEEE ComSoc Excellent Editor Award for IEEE Transactions on Wireless Communications in 2009. His main research interests include B3G technology in wireless communications such as MIMO, OFDM, Multicarrier CDMA , Space Time Coding, and LDPC design etc, Network Coding, Network Information Theory and Cross Layer Design etc.

Dapeng Wu received B.E. in Electrical Engineering from Huazhong University of Science and Technology, Wuhan, China, in 1990, M.E. in Electrical Engineering from Beijing University of Posts and Telecommunications, Beijing, China, in 1997, and Ph.D. in Electrical and Computer Engineering from Carnegie Mellon University, Pittsburgh, PA, in 2003.

Since 2003, he has been on the faculty of Electrical and Computer Engineering Department at University of Florida, Gainesville, FL, where he is currently Professor; previously, he was Assistant Professor from 2003 to 2008, and Associate Professor from 2008 to 2011. His research interests are in the areas of networking, communications, signal processing, computer vision, and machine learning. He received University of Florida Research Foundation Professorship Award in 2009, AFOSR Young Investigator Program (YIP) Award in 2009, ONR Young Investigator Program (YIP) Award in 2008, NSF CAREER award in 2007, the IEEE Circuits and Systems for Video Technology (CSVT) Transactions Best Paper Award for Year 2001, and the Best Paper Award in International Conference on Quality of Service in Heterogeneous Wired/Wireless Networks (QShine) 2006.

Currently, he serves as an Associate Editor for IEEE Transactions on Circuits and Systems for Video Technology, Journal of Visual Communication and Image Representation, and International Journal of Ad Hoc and Ubiquitous Computing. He was the founding Editor-in-Chief of Journal of Advances in Multimedia between 2006 and 2008, and an Associate Editor for IEEE Transactions on Wireless Communications and IEEE Transactions on Vehicular Technology between 2004 and 2007. He is also a guest-editor for IEEE Journal on Selected Areas in Communications (JSAC), Special Issue on Cross-layer Optimized Wireless Multimedia Communications. He will serve as Technical Program Committee (TPC) Chair for IEEE INFOCOM 2012, and has served as TPC Chair for IEEE International Conference on Communications (ICC 2008), Signal Processing for Communications Symposium, and as a member of executive committee and/or technical program committee of over 50 conferences. He has served as Chair for the Award Committee, and Chair of Mobile and wireless multimedia Interest Group (MobIG), Technical Committee on Multimedia Communications, IEEE Communications Society.

DOI: 10.1002/wcm